https://doi.org/10.15407/cryo35.02.076
UDC 601.2:611.018.82.088.5:57.086.13

**O.M. Sukach *, I.F. Kovalenko, S.V. Vsevolodska, O.V. Ochenashko, S.E. Kovalenko**
Institute for Problems of Cryobiology and Cryomedicine of the National Academy of Sciences of Ukraine, Kharkiv, Ukraine
*an_sukach@ukr.net

# THEORETICAL DETERMINATION OF BIOPHYSICAL PARAMETERS FOR OPTIMISING NEURAL CELLS' THREE-DIMENSIONAL STRUCTURES CRYOPRESERVATION

*Using physical and mathematical modelling of the mass transfer processes of water and $Me_2SO$, the values of the relative osmotically inactive volume for aggregates and spheroids of neural cells from newborn rats were determined. The evaluated parameters for aggregates and spheroids are 0.689 and 0.644, respectively. The study also presents theoretically calculated changes over time in the normalized osmotic pressure of $Me_2SO$ and the concentration of salt ions within spheroids and aggregates. From the dynamic curves of change in relative volume for aggregates and spheroids, the filtration coefficients for water and permeability for $Me_2SO$ were determined. It was found that aggregates, as less densely packed structures than spheroids, were characterised by higher permeability coefficients for water and $Me_2SO$, particularly at 5 °C. At this temperature, 119 s is required for 95% saturation of aggregate cells with 10% $Me_2SO$ and 157 s for spheroid. This means that at a temperature of 5 °C, the equilibration time with the cryoprotectant $Me_2SO$ is 25% longer for spheroids than for aggregates. The obtained results indicate that spheroids as a more integral structure characterised by dense cell-cell and cell-extracellular matrix interactions, are more osmotically active compared to aggregates. These findings can be used to develop the optimal methods for cryopreservation of neural cell aggregates and spheroids.*

***Key words:*** *neural cells, spheroids, aggregates, cultivation, filtration coefficients, permeability coefficients, dimethyl sulfoxide, osmotically inactive volume.*

Despite significant scientific efforts, our understanding of how the brain works, both in health and in disease, remains very limited. This is mainly due to the complexity of the structure and functioning of the mammalian nervous system, as well as the limited access to brain tissue directly. In view of this, three-dimensional (3D) neural cell (NCs) cultures, which are a simplified and accessible model of the brain tissue, open up new opportunities for further study of the brain physiology of living organisms. Unlike 2D culture models, 3D culture systems allow to reproduce the complex microenvironment surrounding NCs, including the extracellular matrix and extracellular interactions [3].

The widespread use of 3D NC structures in scientific research is largely limited by the lack of effective protocols for their cryopreservation. The development of low-temperature banks of standardized 3D structures of NCs can expand the possibilities for their use in biomedical and pharmacological research, and will also help to reduce the number of experimental studies involving laboratory animals [2].

Reference: Sukach OM, Kovalenko IF, Vsevolodska SV, Ochenashko OV, Kovalenko SE. Theoretical determination of biophysical parameters for optimising neural cells' three-dimensional structures cryopreservation. *Probl Cryobiol Cryomed*. 2025; 35(2): 76–84. https://doi.org/10.15407/cryo35.02.076

It should be noted that the 3D nature of these multicellular structures complicates their cryopreservation process compared to suspensions of single cells. It introduces additional factors that should be considered when developing relevant cryopreservation protocols, including the rate of cell saturation with a cryoprotectant, the uniformity of their cooling, and the homogeneity of crystal formation.

The use of a physical-mathematical model describing mass transfer processes to record changes in the relative volume of NCs during their incubation in a cryoprotective solution allows to determine the optimal exposure time of NCs with a cryoprotectant and the optimal cooling rate for successful cryopreservation of a cell suspension [6]. The same approach can be used to determine the exposure time to a cryoprotectant and the optimal cooling rate for cells in 3D structures. Meanwhile, the integral characteristics that determine the time parameters of mass transfer between 3D structures and the medium can be considered as analogues of the permeability coefficients of individual cell membranes.

Neural cells are capable of forming different types of multicellular 3D structures: neurospheres, aggregates (AGs), and spheroids (SPHs), which differ somewhat in their morphological and physiological characteristics. Neurospheres are formed by neural stem cells during their cultivation [10], and aggregates are formed by self-assembling a heterogeneous suspension of freshly obtained NCs during short-term cultivation [11, 12]. Spheroid formation occurs when pre-cultured NCs are grown on non-adherent surfaces or in a droplet (also by self-assembling) [4]. Morphologically, these structures are similar, but they differ in their formation method, cell composition, and, possibly, extracellular matrix content. This means that the conditions for both cryoprotectant saturation of these 3D structures and their cooling rates are likely to be different. To develop effective cryopreservation protocols for different types of 3D NCs structures, it is necessary to determine their biophysical parameters, in particular the filtration coefficients for water and the permeability coefficients for $Me_2SO$.

The purpose of this work is to determine, based on physico-mathematical modeling of the osmotic activity of aggregates and spheroids, their filtration coefficients for water and permeability for $Me_2SO$, as well as the optimal time required for the saturation of their cells with $Me_2SO$.

## MATERIAL AND METHODS

The primary suspensions, aggregates and spheroids of the NCs from newborn rats were used in the study.

Neural cells were obtained from the brain tissue of newborn rats (Postnatal day 0) by the enzymatic-mechanical method. For this purpose, the brain tissue was removed, washed with sterile saline, incubated for 2 min at 37 °C in 0.25% trypsin solution (Biowest, France), transferred to DMEM/F12 medium (Biowest, France) enriched with 10% serum and mechanically disaggregated into single cells by vibration [9]. The obtained cell suspension was filtered and washed from trypsin by centrifugation at 100 g. The resulting cell pellet was suspended in DMEM/F12 medium supplemented with 10% blood serum. Cell viability was assessed by staining with 0.4% trypan blue (Sigma, USA). The number of cells was counted in a Goryaev chamber.

Primary suspensions of NCs with viability above 70% were used in the study. Monolayer and 3D cultivations were carried out in a $CO_2$ incubator at 37 °C, 5% $CO_2$ atmosphere, 95% air in DMEM/F12 medium (Biowest, France), supplemented with 10% blood serum.

To obtain AGs, the primary suspension of NCs was seeded at a concentration of $4 \times 10^6$ cells/ml in a 24-well plate (TPP, Switzerland) and cultured for 1—3 h [11]. A portion of the formed AGs was reseeded in a minimal volume and cultured in the same medium until a 70% monolayer was formed. The NCs of the monolayer were removed with a solution of trypsin (0.25%)/versen (0.05%) (Biowest, France), washed by centrifugation, resuspended in the culture medium and used in further experiments to obtain SPHs.

NC spheroids were obtained by the hanging drop culture technique. For this purpose, culture dishes with a diameter of 100 mm (SPL Life Sciences, South Korea) were used. Drops of pre-cultured NCs were applied to the inner surface of the lid, and the bottom of the dish was filled with a sterile solution to maintain humidity in the chamber. Each drop was 20 μL and contained $8 \times 10^3$ cells. The culture dishes with drops were cultured in a $CO_2$ incubator at 37 °C in an atmosphere of 5% $CO_2$, 95% air for 3—4 days until spheroids were formed. Spheroids formation was evaluated by inverted microscope (AmSCOPE, USA). The viabil-

ity of NCs in the SPHs was assessed by culturing on the adhesive surface of 24-well plates.

The determination of the integral permeability coefficients of SPH and AG for the penetrating cryoprotectant $Me_2SO$ — Ks, and for water molecules – Lp, was carried out using the volumetric method [1, 2]. The volumes of SPH and AG before ($V_0$) and after (V) the addition of solutions were determined by the formula:

$$V = 1/6\ \pi D^3,$$

where D is the diameter of SPH and AG.

The volume of SPH and AG was determined using an «Axio Observer Z1» microscope (Carl Zeiss, Germany) equipped with a thermostated stage.

Morphometric analysis was performed using the certified software 'AxioVision Rel. 4.8 (Carl Zeiss, Germany).

The osmotically inactive volume of SPH and AG was determined by the method described in the work of V.V. Ogurtsova *et al.* [8]. For this purpose, the dependence of their relative volume on the inverse normalized osmotic pressure in sodium chloride solutions at concentrations of 0.5, 1, and 2.0 mol/L was determined.

Considering the volume of SPHs and AGs in a series of solutions of a non-penetrating substance with increasing concentration, the dependence of the asymptotic relative volume on the inverse normalized osmotic pressure of the solution was found. The experimental data were approximated by the least squares method. The value of the osmotically inactive volume was obtained from the intersection of the approximated line with the ordinate axis.

The numerical values of the integral filtration and $Me_2SO$ permeability coefficients in SPH and AG were determined by approximating the experimental data on the change in their relative volume depending on the exposure time in the studied solutions. This was done using theoretical curves calculated on the basis of the Kedem-Katchalsky physico-mathematical model of passive transport of water and penetrating substances, ensuring their maximum congruence [5, 7].

In dimensionless form, the classical Kedem-Katchalsky model is expressed as follows

$$\begin{cases} \dfrac{dy}{dt} = \dfrac{1}{\tau_0}\left[\sigma_1(\hat{\pi}_1^{in} - \hat{\pi}_1^{out}) + \dfrac{1-\alpha}{y-\alpha} - 1\right], & (1) \\ \dfrac{d\hat{\pi}_1^{in}}{dt} = \dfrac{1}{\tau_1}\left[(\hat{\pi}_1^{in} - \hat{\pi}_1^{out}) + \sigma_1\hat{\pi}_1^{in}\dfrac{dy}{dt}\right]\dfrac{1}{y-\alpha}, & (2) \\ \hat{\pi}_2^{in} = \hat{\pi}_2^{in}(0)\left(\dfrac{1-\alpha}{y-\alpha}\right), & (3) \end{cases}$$

where $y = \frac{V}{V_0}$ ($V$ and $V_0$ — the current and initial volumes of SPHs and AGs, respectively); $\tau_0 = \frac{1}{7{,}8 L_p y_0}$ (7,8 — osmotic pressure coefficient of the isotonic solution in atmospheres), $L_p$ — the integral filtration coefficient of SPH and AG, $\gamma_0$ — the surface-to-volume ratio of a cell, $\gamma_0 = S_0/V_0$, $S_0$ — the initial surface area of the cell membrane); $t$ — time; $\sigma_1$— the reflection coefficient of the plasma membrane for the substance penetrating it; $\hat{\pi}_{1,2}^{in,\ out} = \pi_{1,2}^{in,\ out}/\pi_0$ — normalized osmotic pressure of the permeable (1) and impermeable (2) components inside and outside the cell; $\pi_1^{out}$ and $\pi_1^{in}$ — osmotic pressure of the substance penetrating the plasma membrane, outside and inside the cell, respectively; – the initial value of the osmotic pressure of the isotonic physiological solution; $\tau_1 = \frac{1}{K_S y_0}$ (where $K_S$ — the permeability coefficient of the plasma membrane for the substance penetrating it); $a$ — the volume fraction of osmotically inactive intracellular substances.

The reflection coefficient of the cell membrane σ1 was assumed to be 0.95 in all calculations. The cell membrane permeability coefficients were calculated by solving the system of differential equations (1)—(3).

Statistical analysis of the obtained results was performed using the non-parametric Mann-Whitney U test with the software «Statgraphics plus for Windows 2.1» (Manugistics Inc., USA). The experimental data are presented as mean ±SD. Differences were considered significant at $p \le 0.05$.

## RESULTS

Permeability parameters were determined in 3D NC structures: aggregates (Fig. 1, *a*) and spheroids (Fig. 1, *b*), which consisted of viable cells. This is evidenced by their ability to attach to an adhesive surface during cultivation, followed by cell migration and spreading (Fig. 1, *c*, *d*).

Permeability parameters were determined for SPH and AG with a diameter of 200—300 μm. Changes in the volume of SPH and AG during their equilibration in a 10% $Me_2SO$ physiological solution at temperatures of 5, 15, 25 and 35 °C were determined by morphometric analysis of micrographs (Figs 2, 3).

Based on the data obtained by the method of V.V. Ogurtsova *et al.* [3], a graph was plotted showing the changes in the relative volume of SPH and AG depending on the reciprocal normalized osmotic pressure of the NaCl solution (Fig. 4).

The graph shows that the relative osmotically inactive volume (α) of SPH and AG differs. For

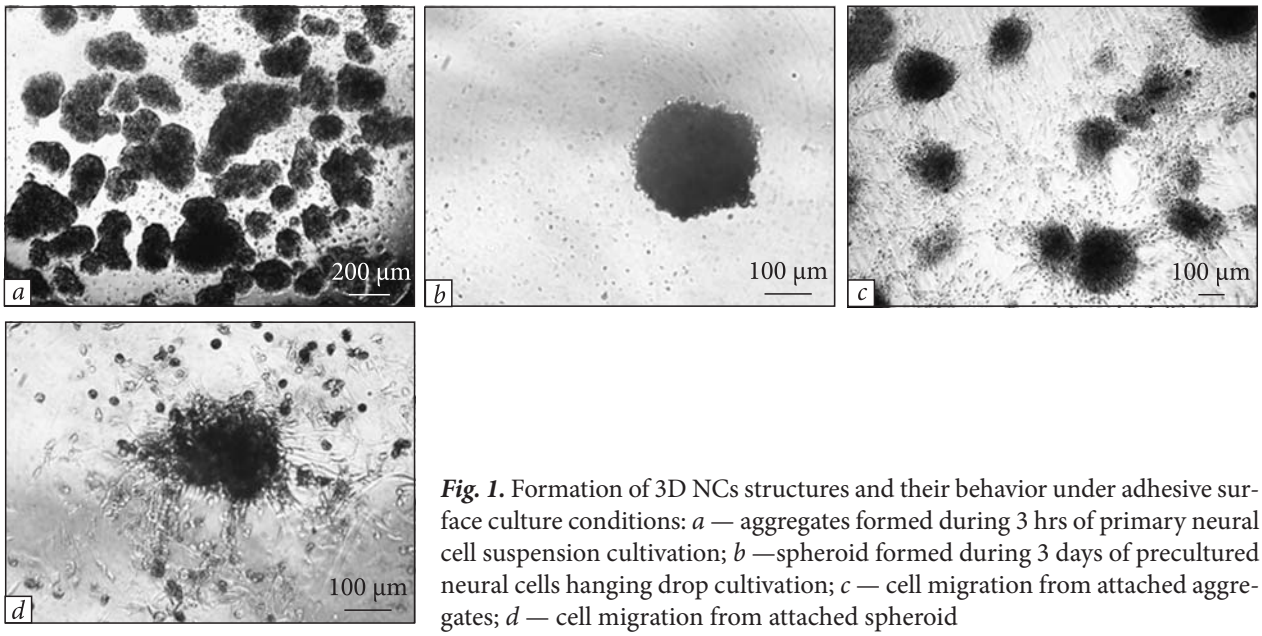


***Fig. 1.*** Formation of 3D NCs structures and their behavior under adhesive surface culture conditions: *a* — aggregates formed during 3 hrs of primary neural cell suspension cultivation; *b* —spheroid formed during 3 days of precultured neural cells hanging drop cultivation; *c* — cell migration from attached aggregates; *d* — cell migration from attached spheroid

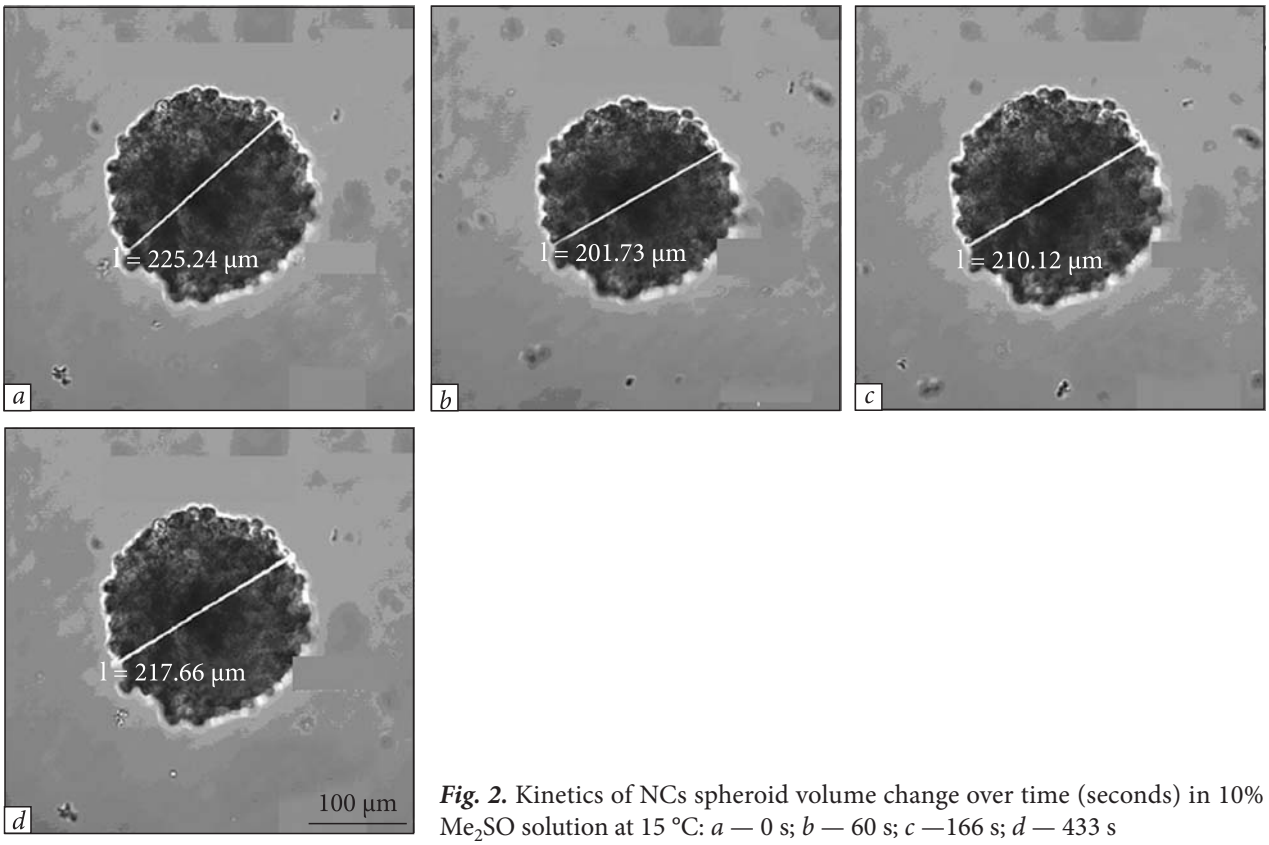


***Fig. 2.*** Kinetics of NCs spheroid volume change over time (seconds) in 10% $Me_2SO$ solution at 15 °C: *a* — 0 s; *b* — 60 s; *c* —166 s; *d* — 433 s

SPH, it is 0.644, while for AGs it is 0.689. This means that the reaction of SPH and AG to the same hypertonic effect is not the same, which may indicate a different volume fraction of osmotically inactive substance inside these multicellular structures [7]. The reasons for this difference may also be the origin and structure of the osmotically inactive extracellular matrix, cellular composition, and the different duration of SPH and AG cultivation.

Aggregates are looser multicellular structures compared to spheroids. As seen in Fig. 1, *a* and 3, aggregates contain a rather large amount of extracellular substance, which evidently originates from

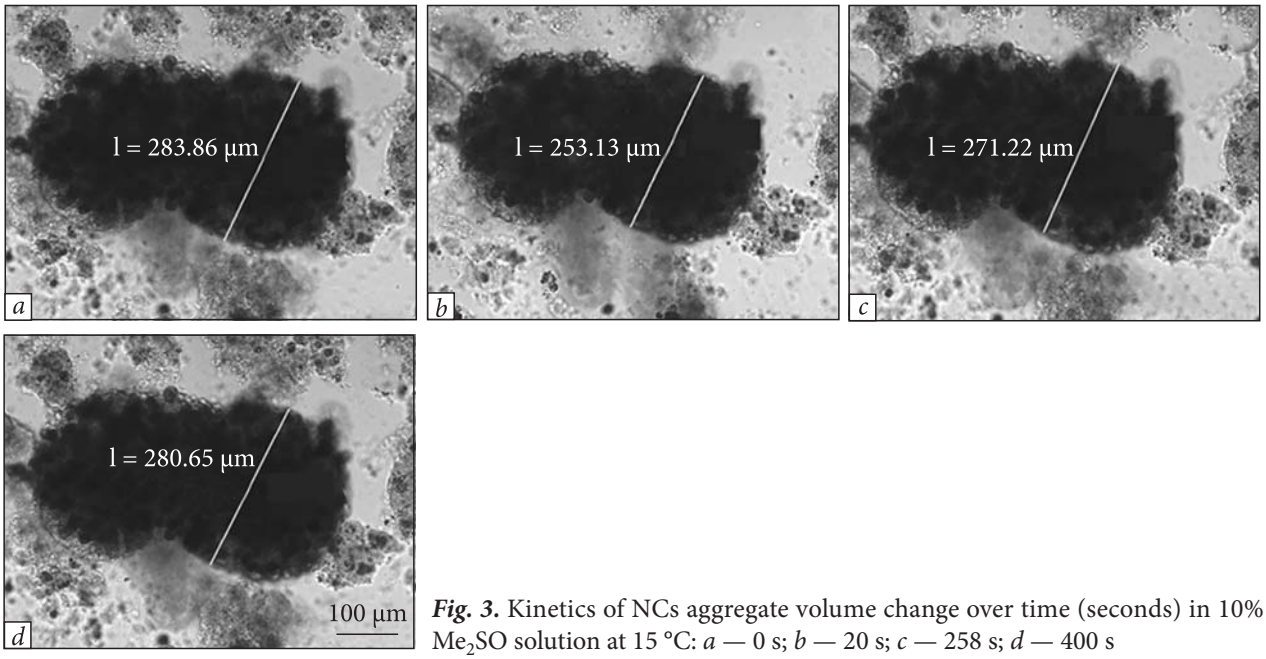


***Fig. 3.*** Kinetics of NCs aggregate volume change over time (seconds) in 10% $Me_2SO$ solution at 15 °C: *a* — 0 s; *b* — 20 s; *c* — 258 s; *d* — 400 s

the initial tissue. Spheroids, unlike aggregates, are structures with a denser cell packing (Fig. 1, *b*, 2) and a tighter intercellular matrix, which is a product of spheroid cell metabolism. This matrix is quite tightly bound to the cells, unlike the aggregate's exogenous extracellular matrix, whose connection to the cells is likely absent due to the short cultivation period.

Thus, a spheroid is a more integral structure compared to an aggregate, where the cells and the extracellular matrix do not form a single unit and therefore react to osmotic changes separately. Since the extracellular matrix is osmotically inactive, it dampens the osmotic changes of NCs within aggregates, and we are not able to fully observe the volume changes of aggregate cells. Spheroids, as a structure with dense cell-extracellular matrix interactions, respond to osmotic changes as an integral system, which allows for more accurate tracking of the cells' reaction to the effect of an impermeable extracellular fluid.

It is important to emphasize that the diffusion of water and cryoprotectant molecules in 3D multicellular structures is not solely a function of cell membrane permeability but also depends significantly on extracellular diffusion. This, in turn, is determined by the cell packing density, as well as the volume and structure of the extracellular matrix. Specifically, in spheroids, dense cell packing and the presence of a bound matrix can create diffusion barriers that slow down the transport of $Me_2SO$ molecules into the core of the structure. As a result, the duration of equilibration in such systems is determined not only by membrane permeability but also by the effective coefficient of extracellular diffusion. Consequently, AGs show a greater relative increase in volume during equilibration compared to SPHs, and their volumetric stabilization occurs more rapidly. This also aligns with the faster uptake of cryoprotectant by AG cells, which may be relevant for optimizing cryoprotection protocols in relation to the morphological features of 3D structures. Consequently, the relative volume increase of AGs during equilibration is higher than in SPHs, and volume stabilization in AGs occurs faster. This fact also cor-

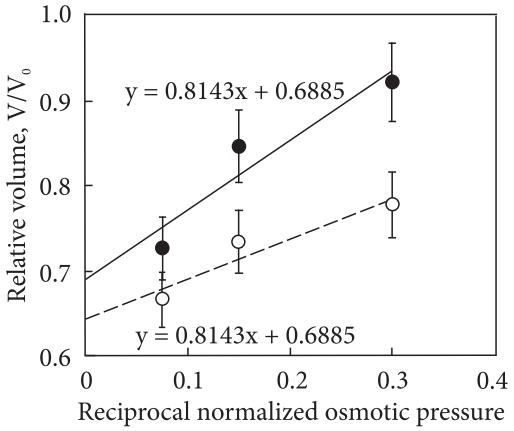


***Fig. 4.*** Changes in relative volume of AG (•) and SPH (◦) depending on reciprocal normalized osmotic pressure of NaCl solution

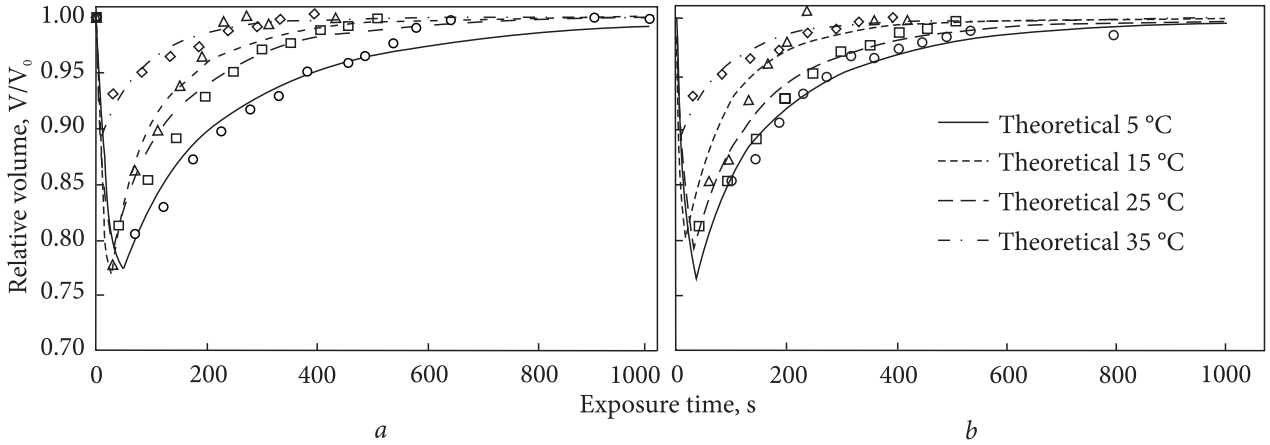


***Fig. 5.*** Changes over time in the relative spheroids (*a*) and aggregates (*b*) volume during its equilibration in 10% $Me_2SO$ at various temperatures: ○ — 5 °C; □ — 15 °C; Δ —25 °C; ◊ —35 °C

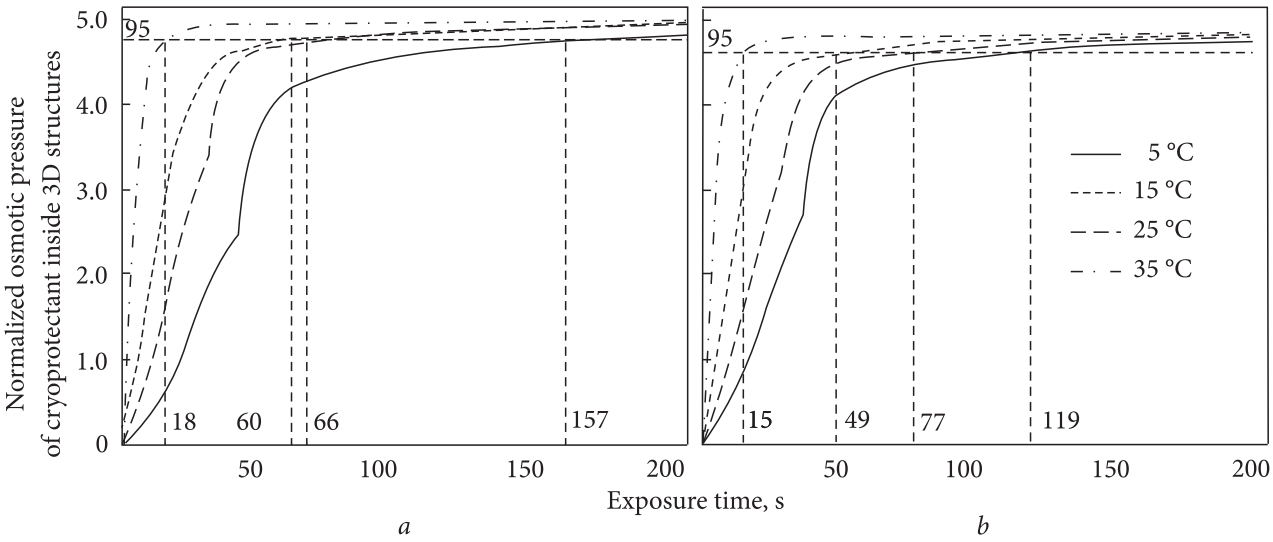


***Fig. 6.*** Time-dependent changes in the concentration of $Me_2SO$ inside spheroids (*a*) and aggregates (*b*) at equilibration temperatures

relates with the more rapid saturation of AG cells with the cryoprotectant, which may be significant for optimizing cryopreservation protocols depending on the morphological features of the 3D structures.

Thus, the observed differences in the time of $Me_2SO$ uptake by the multicellular structures, interpreted on the basis of the Kedem—Katchalsky model parameters, may be determined not only by transmembrane permeability but also by concentration gradients in the intercellular space. Particularly in dense structures such as spheroids, it should be taken into account that extracellular diffusion represents the rate-limiting step, and adsorption effects or changes in the local chemical potential may influence the overall mass transfer kinetics.

The different osmotic activity of SPHs and AGs is also indicated by diagrams showing time-dependent changes in relative volume during incubation in a 10% $Me_2SO$ solution (Fig. 5). The graph shows that SPH cells dehydrate and recover their volume more slowly than AG cells during equilibration in a 10% $Me_2SO$ solution at various temperatures.

Fig. 6 and 7, and Table present the theoretically calculated time-dependent changes in the normalized osmotic pressure of $Me_2SO$ and the concentration of salt ions inside SPH and AG, based on equations (1)—(3).

As seen in Fig. 6, theoretical calculations show that (157± 20), (66 ± 9), (60 ± 6) and (18 ± 5) s are sufficient for 95% saturation of SPH cells with cryoprotectant during their equilibration in a 10%

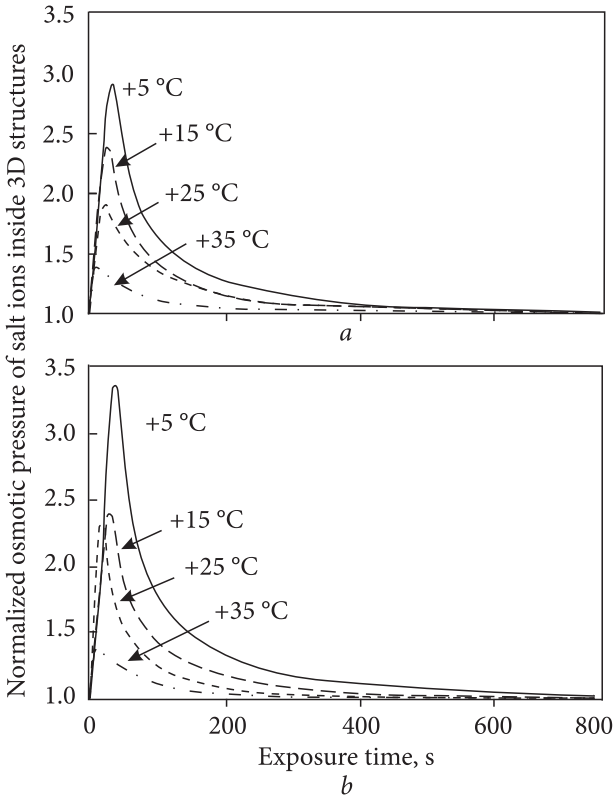


***Fig. 7.*** Time-dependent changes in the normalized salt ion concentration inside spheroids (*a*) and aggregates (*b*) at equilibration temperatures of 5, 15, 25, and 35 °C

$Me_2SO$ solution at 5, 15, 25 and 35 °C, respectively. For AG cells, the corresponding times are (119 ± ± 16), (77 ± 7), (49 ± 6), and (15 ± 6) s, respectively. This means that AG cells require less equilibration time in a 10% $Me_2SO$ solution to achieve cryoprotectant saturation than SPH cells. This difference becomes more pronounced as the incubation temperature decreases. Specifically, at 5 °C, AG cells require 25% less time for $Me_2SO$ saturation compared to SPH cells. This fact should be taken into account during the cryopreservation of AGs and SPHs.

As seen in Fig. 7, the theoretically calculated concentration of salt ions inside AG is slightly higher than in SPH cells. This difference is particularly pronounced at 5 °C. This indicates that the dehydration rate of AG cells is higher than that of SPH cells in this case, which can be explained by the different packing densities of SPH and AG, as well as by the higher permeability coefficients for water and $Me_2SO$ in AG cells.

The table presents the calculated integral filtration coefficients ($L_p$) for water and permeability coefficients ($K_s$) for $Me_2SO$ molecules of cell membranes within SPHs and AGs.

As can be seen from the Table data, the magnitude of the filtration coefficients for water and the permeability coefficients for $Me_2SO$ in SPHs and AGs is directly proportional to temperature. It should be noted that at all the studied temperatures, these coefficients are higher for AGs than for SPHs.

The $Me_2SO$ permeability coefficients are 1.1–5.8 times higher for AGs compared to SPHs (Table). The maximum difference in this parameter for AGs and SPHs was recorded at 35 °C. This is likely related to the cell packing density in the 3D structures, which is significantly higher in SPHs than in AGs, as well as the presence of a dense extracellular matrix in the intercellular space of SPHs, which forms during their development. Both dense intercellular contacts and the extracellular matrix contribute to a reduced diffusion rate for both water and $Me_2SO$ molecules into the cells of the inner layers of SPHs, compared to the same cells in AGs.

From the Table, it is evident that the values of the water filtration coefficients for AGs are also significantly higher (2.3—3.9 times) than for SPHs. Furthermore, this increase is greater at lower temperatures (Table). This fact is quite difficult to explain, but a possible reason is the experimental conditions, which do not allow for the recording of biological objects from the first seconds of the study. An explanation for this relationship requires additional investigation.

**Filtration coefficients for water and permeability coefficients for $Me_2SO$ of cell membranes in spheroids and aggregates depending on the different temperatures, n = 5**

| Object of study | Coefficients | Temperature, °C | | | |
|---|---|---|---|---|---|
| | | 5 | 15 | 25 | 35 |
| Spheroid | Filtration $L_p \times 10^{14}$, $m^3/N \cdot s$ | 0.91 ± 0.25 | 1.25 ± 0.07 | 1.91 ± 0.19 | 2.14 ± 0.18 |
| | Permeability $K_s \times 10^6$, m/s | 0.29 ± 0.11 | 1.06 ± 0.11 | 1.24 ± 0.29 | 1.43 ± 0.18 |
| Aggregate | Filtration $L_p \times 10^{14}$, $m^3/N \cdot s$ | 3.52 ± 0.62 # | 4.14 ± 0.78 # | 4.7 2 ± 0.28 # | 5.01 ± 0.62 # |
| | Permeability $K_s \times 10^6$, m/s | 0.32 ± 0.03 | 2.06 ± 0.54 * | 4.62 ± 0.78 * | 8.33 ± 0.87 * |

Notes: # changes are significant compared to $L_p$ SPH, $p \le 0.05$; * changes are significant compared to $K_s$ SPH, $p \le 0.05$.

Thus, the conducted studies have shown that the extracellular matrix content and the cell-cell and cell-extracellular matrix interactions (cell packing density), which differ significantly between spheroids and aggregates, have a major impact on the diffusion of water and $Me_2SO$ molecules into the cells of these 3D structures.

The obtained data on the permeability of neural cells within SPHs and AGs can be used to develop the optimal cryopreservation protocols, particularly for determining the optimal equilibration time of these multicellular structures in cryopreservation media at different temperatures.

Therefore, for a more detailed clarification of the permeability mechanisms of NCs within SPHs and AGs to water and $Me_2SO$ molecules, further research is necessary.

## CONCLUSIONS

1. Spheroids of neural cells, as a more integral 3D structure with dense cell-cell and cell-extracellular matrix interactions, demonstrate higher osmotic activity compared to aggregates. This is confirmed by the spheroids' smaller relative osmotically inactive volume (0.644) versus 0.689 for NC aggregates.

2. Neural cell aggregates, which are less densely packed structures compared to spheroids, are characterized by higher permeability coefficients for water and $Me_2SO$. This is particularly evident at 5 °C. At this temperature, 95% saturation of AG cells with a 10% $Me_2SO$ solution requires 25% less time than for SPH cells (119 s versus 157 s).

3. Osmotic and diffusive processes in aggregates and spheroids are influenced not only by the properties of cell membranes but also by cell packing density, the structural organization of the extracellular matrix, and the efficiency of extracellular diffusion. These factors should be taken into account when modeling the cryopreservation of volumetric cell structures. To better delineate the effects of membrane permeability and extracellular diffusion, it is advisable to introduce normalized coefficients based on density or volume fraction of the matrix.

REFERENCES

1. Andrews MG, Kriegstein AR. Challenges of organoid research. Annu Rev Neurosci. 2022; 45: 23–39.
2. Bédard P, Gauvin S, Ferland K, et al. Innovative human three-dimensional tissue-engineered models as an alternative to animal testing. Bioengineering (Basel) [Internet]. 2020 Sep 17 [cited 2025 May 20]; 7(3): 115. Available from: https://www.mdpi.com/2306-5354/7/3/115
3. Cho AN, Jin Y, An Y, et al. Microfluidic device with brain extracellular matrix promotes structural and functional maturation of human brain organoids. Nat Commun [Internet]. 2021 Aug 05 [cited 2025 May 20]; 12(1): 4730. Available from: https://www.nature.com/articles/s41467-021-24775-5
4. Dingle YT, Boutin ME, Chirila AM, et al. Three-dimensional neural spheroid culture: an in vitro model for cortical studies. Tissue Eng Part C Methods. 2015; 21(12): 1274—83.
5. Gordiyenko YeO, Gordiyenko OI, Maruschenko VV, Sakun OV. [Improved model for the passive mass transfer through the cell plasma membrane]. Biophysical Bulletin. 2008; 21(2): 75—80. Ukrainian
6. Gordiyenko OI, Kovalenko SYe, Kovalenko IF, et al. Theoretical estimation of the optimum cooling rate of a cell suspension at linear freezing modes based on a two-factor theory of cryodamage. CryoLetters. 2018; 39(6): 380—5.
7. Gordiyenko YeO, Pushkar NS. [Physical basis for low temperature preservation of cell suspensions]. Kyiv: Naukova dumka; 1994. 140 p. Russian
8. Ogurtsova VV, Kovalenko SYe, Kovalenko IF, Gordiyenko OI. Determination of osmotically inactive volume of murine enterocytes. Probl Cryobiol Cryomed. 2016; 26(1): 93—7.
9. Petrenko AYu, Sukach AN. Isolation of intact mitochondria and hepatocytes using vibration. Analytical Biochem. 1991; 194(2): 326—9.
10. Reynolds BA, Rietze RL. Neural stem cells and neurospheres – reevaluating the relationship. Nat Methods. 2005; 2: 333—6.
11. Sukach AN, Liashenko TD, Shevchenko M.V. Properties of isolated neural cells from newborn rat in tissue in vitro. Biotechnologia Acta. 2013; 6(3):63—8.
12. Sukach OM, Vsevolodska SO, Ochenashko OV, Shevchenko MV. Obtaining and characterization of rat fetuses neural cells aggregates/spheroids. Biopolym Cell. 2022; 38(2): 93—102.

Received 20.11.2024
Accepted for publication 19.06.2025

*О.М. Сукач *, І.Ф. Коваленко, С.В. Всеволодська, О.В Оченашко, С.Є. Коваленко*
Інститут проблем кріобіології та кріомедицини НАН України
м. Харків, Україна
* an_sukach@ukr.net

ТЕОРЕТИЧНЕ ВИЗНАЧЕННЯ БІОФІЗИЧНИХ ПАРАМЕТРІВ ТРИВИМІРНИХ СТРУКТУР НЕЙРАЛЬНИХ КЛІТИН З МЕТОЮ ОПТИМІЗАЦІЇ ЇХ КРІОКОНСЕРВУВАННЯ

У роботі з використанням фізико-математичного моделювання процесів масопереносу води і ДМСО визначено величини відносного осмотично неактивного об'єму для агрегатів і сфероїдів нейральних клітин новонароджених щурів. Досліджувані параметри для агрегатів і сфероїдів складають 0,689 і 0,644 відповідно. Також у роботі представлені теоретично розраховані зміни у часі приведеного осмотичного тиску ДМСО та концентрації іонів солей всередині агрегатів і сфероїдів. З динамічних кривих зміни відносного об'єму для агрегатів та сфероїдів визначено коефіцієнти фільтрації для води та проникності для ДМСО. Виявлено, що агрегати, які є менш щільно упакованими структурами порівняно зі сфероїдами, мають більші коефіцієнти проникності для води і ДМСО, що особливо проявляється при 5 °С. За цієї температури для 95%-го насичення кріопротектором клітин під час інкубації агрегатів у 10%-му розчині ДМСО необхідно 119 с, сфероїдів — 157 с. Тобто при температурі 5 °С тривалість еквілібрації з кріопротектором ДМСО для сфероїдів є на 25 % більшою, ніж для агрегатів. Отримані дані вказують на те, що сфероїди, які є більш цілісними структурами зі щільними зв'язками клітин з матриксом та клітин між собою, більш осмотично активні порівняно з агрегатами. Результати проведеного дослідження можуть бути використані для розробки оптимальних режимів кріоконсервування агрегатів та сфероїдів нейральних клітин.

***Ключові слова*:** нейральні клітини, сфероїди, агрегати, культивування, коефіцієнти фільтрації, коефіцієнти проникності, диметилсульфоксид, осмотично неактивний об'єм.